GSC Advanced Research and Reviews

eISSN: 2582-4597 CODEN (USA): GARRC2

Cross Ref DOI: 10.30574/gscarr

Journal homepage: https://gsconlinepress.com/journals/gscarr/

(RESEARCH ARTICLE)

Check for updates

Textural, mineralogical and physico-chemical characterization of red clay of Tanout (Zinder-Niger) with a view to its valorization in water treatment

Rabilou Souley Moussa [1,*], Ousmaila Sanda Mamane [2], Issa Habou [1], Maman Mousbahou Malam Alma [1] and Ibrahim Natatou [1]

[1] *Department of chemistry, Faculty of Science and Technology, Abdou Moumouni University of Niamey, B. P: 10662 Niamey, Niger.*

[2] *Department of chemistry, Faculty of Science and Technology, University of Agadez, B.P: 199 Agadez, Niger.*

GSC Advanced Research and Reviews, 2022, 13(03), 039–053

Publication history: Received on 20 October 2022; revised on 27 November 2022; accepted on 30 November 2022

Article DOI: https://doi.org/10.30574/gscarr.2022.13.3.0339

Abstract

This study aims to determine the textural (specific surface, pore volume and pore size) and mineralogical characteristics of Tanout red clay of Zinder region (Niger) in order to have textural data allowing its use as an adsorbent. The methodology is based on textural analyzes (adsorption of N_2 at 77 K by the Brunauer-Emmett-Teller method), mineralogical (X-ray fluorescence, X-ray diffraction, thermo-gravimetric analysis, scanning electron microscopy) and physicochemical (preliminary analyses). The results obtained show that the red clay has a specific surface of 418.4 $m^2.g^{-1}$ and 967.7 $m^2.g^{-1}$ calculated according to the BET and Langmuir methods respectively and a microporous surface of 540 m2.g- 1, with pore volume varying from 0.0389 to 0.2535 $cm^3.g^{-1}$ and pore size varying from 0.3675 to 5.423 nm calculated according to the methods (Barrett-Joyner-Halenda, Dubinin-Radushkevich, Dubinin -A, Horvath-Kawazoe and Saito-Foley). It has slit and cylindrical micro- pores. It has a slightly neutral pH in an aqueous medium and a high cation exchange capacity with low humidity and density, and is mainly composed of SiO_2 (83.2%), Al_2O_3 (7.04%) and Fe_2O_3 (3.35%) with trace elements, the main ones being: Zr (2490 ppm), Sr (310.21 ppm), Cu (310.1 ppm), V (290.1 ppm) and Zn (140ppm). It consists essentially of Montmorillonite, illite and Kaolinite with impurities such as quartz and rutile. This clay has a high degree of crystallinity. These characteristics make it a promoter material that can be used as an adsorbent.

Keywords: Red clay; Textural data; Microporous surface; Tanout; Zinder

1. Introduction

In a context of constantly increasing and uncontrolled pollution, we are witnessing deterioration in the physicochemical quality of consumption water due to pollutants of geogenic and anthropogenic origin. In Niger, recent studies on the characterization of groundwater in certain aquifers in Zinder region have shown water pollution by fluoride, nitrate and nitrite ions in certain structures [1, 2, 3]. While access to consumption water in an equitable, safe and affordable way is a right for all, as advocated by the World Health Organization [4]. Indeed, to solve the problem of polluted consumption water, numerous research works have shown the use of clay materials in depollution. But, in Niger, this domain remains in a stationary state where we note only the study carried out on the adsorption of fluoride ions by a bentonite from Niger [5] and the study on the valorization of two clay materials from the valley of the Niger River in the elimination of copper from consumption water [6]. However, the use of a natural material as an adsorbent to eliminate pollutants, resides perfectly in the exact knowledge of its physicochemical, mineralogical, structural and textural properties, especially the specific surfaces, the pore volumes and the pore sizes, because these are the determining

* Corresponding author: Rabilou Souley Moussa

Department of chemistry, Faculty of Science and Technology, Abdou Moumouni University of Niamey, B. P: 10662 Niamey, Niger.

factors of a good adsorbent. In Niger, we only note the study on the characterization of a mixed Niger clay in Tahoua region [7] which makes use of these types of properties. It is in this context that this study takes place, the objective of it is to determine the physicochemical, mineralogical, structural and textural characteristics of a red clay of Tanout in Zinder region in order to conclude on its possible use in depollution of consumption water.

2. Material and methods

2.1. Sampling

The red clay sample was taken from a quarry in the urban township of Tanout in Zinder region of Niger (Figure 1). This clay is generally used in the brickyard for the construction of housing. This quarry has geographical coordinates: 08.49467° longitude and 14.59266° latitude. The sample taken is named Arg2-B.

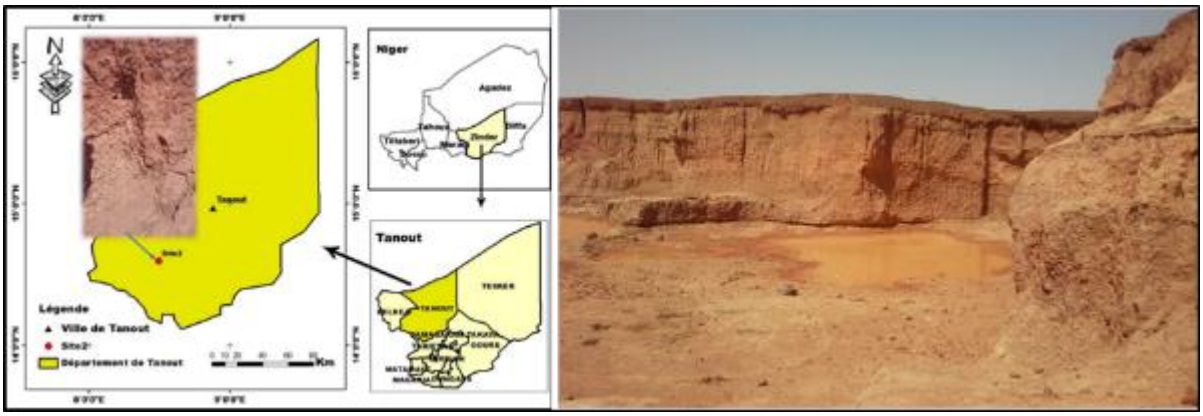

Figure 1 Presentation of the study area and the sampling site

2.2. Crushing, grinding and sieving

The red clay used in this study was crushed, then ground using a jaw crusher and sieved using a 200 µm grain size sieve (Figure 2). This step eliminates a number of impurities such as quartz and reduces the clay into millimetric fragments. These operations were carried out at the Second Year Chemistry Laboratory (LCDA) of the UAM.

Figure 2 Crushing, grinding and sieving red clay

2.3. Process for extracting the clay fraction < 2 µm

This process makes it possible to eliminate certain accessory minerals (quartz, carbonates, feldspar, etc.) and to extract the fine fraction rich in clay minerals. The protocol used was developed by *M. Robert* and *D. Tessier in* [8]. Figure 3 presents the experimental device used. The clay fractions obtained were named Arg2-FNa$^+$ and Arg2-FSNa$^+$.

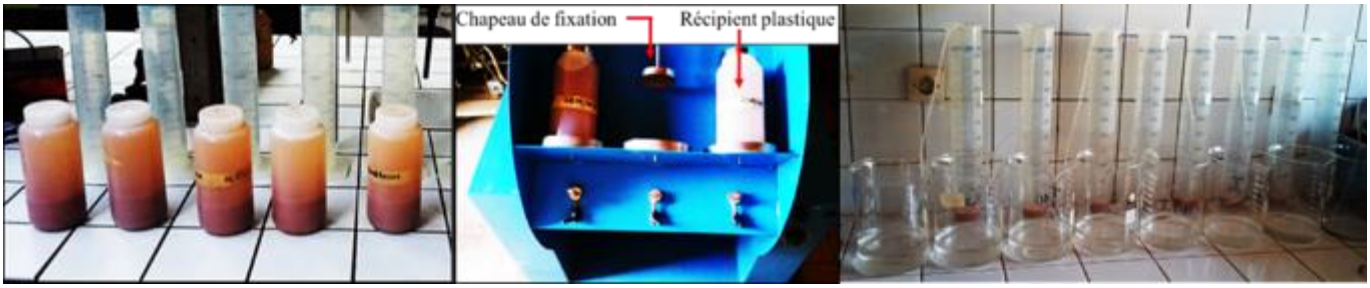

Figure 3 Variable speed eluter (stirring at 34 rpm) and communicating vessel system for the extraction of the fraction < 2 µm

2.4. Red clay pH

The pH was determined to quantify the contribution of acidity when the solid is in contact with the solution. The protocol consists of bringing 1 g of clay into contact with 100 ml of distilled water under magnetic stirring at room temperature for 2 hours. After filtration, the pH of the filtrate was measured. Thus, increasing masses of clays (1, 3 and 5 g) were brought into contact with 50 ml of distilled water under magnetic stirring at room temperature, then the mixture was left to stand for 24 hours with the aim to verify the effect of the clay mass on the pH. Finally, the pH of Arg2-B was measured *AFNOR* in [9].

2.5. Cation exchange capacity (CEC) by conductimetry

The conductometric method has been used to determine the cation exchange capacity of red clay [9, 10]. The protocol consists of putting 1 g of clay in 100 ml of distilled water under magnetic stirring at room temperature for 2h 30 min. After adding 150 ml of a 1 M $BaCl_2$ solution while adjusting the pH to that of the raw clay, the suspension was left under stirring for 2h 30 min. Then the suspension was filtered and washed to a negative $AgNO_3$ test, then oven-dried overnight at 60 °C. After grinding, 0.5 g of treated clay was brought into contact with 50 ml of distilled water under magnetic stirring at room temperature for 2 hours followed by conductometric titration with a 0.02 M $MgSO_4$ solution. At each addition of 0.5 ml of $MgSO_4$ solution, the conductivity value was noted after stabilization. Finally, the curve of conductivity as a function of the volume of $MgSO_4$ poured was plotted and the equivalent point which corresponds to the intersection of two half-lines tangent to the curve was determined. The CEC was calculated by the following formula:

$$CEC\ (meq.100g^{-1}) = 2C\ x\ \frac{V}{m}\ x\ 100\ (1).$$

2.6. Humidity rate

The evaluation of the moisture content can be indicative of the hydrophilic behavior of adsorbent materials. The protocol consists in weighing the empty crucible by noting its weight P, then the hollowed one containing 2 g of clay by noting its weight P_1. The assembly was brought to an oven at 105 °C for 24 hours, then cooled in a desiccator for 30' while again weighing its weight P_2. The moisture content was calculated by the following formula [11].

$$H\ (\%) = \frac{P_1 - P_2}{P_1 - P}\ x\ 100\ (2)$$

2.7. Density

Density is the set of solid and pore fractions. It was determined by the test tube method. This density was calculated by the following formula:

$$\rho\ (g.cm^{-3}) = \frac{P_2 - P_1}{V}(3).$$

2.8. Isoelectric point or pH at point of zero charge (pH_{PCN})

The isoelectric point or pH_{PCN} corresponds to the pH value for which the net charge of the solid surface is zero. The protocol consists of putting 50 mg of clays in 50 ml of distilled water with a pH between 2 and 12 (adjusted by solutions of HCl and 0.01M NaOH) with magnetic stirring at room temperature for 24 hours. Afterwards, the final pH of the suspension was measured and the graph pHf – pHi as a function of pHi was drawn. The isoelectric point corresponds to

the intersection of the curve and the straight line which passes through the origin [12]. This parameter was determined for red clay and its clay fractions < 2 µm.

2.9. Loss on ignition (LOI)

The red clay was subsequently heated to 1000 °C for 2h to determine the LOI. The latter was determined gravimetrically by heating 1 g of powdered clay in a cleaned weighed crucible to 1000 °C. Then the crucible and contents were weighed to obtain the difference in weight before and after heating. The following formula was applied to determine the LOI.

$$LOI = \left(\frac{a-b}{a}\right) x\ 100\ (4).$$

With:
a = weight of the crucible + 1 g of the sample before heating,
b = weight of the crucible + 1 g of the sample after heating.

The analysis was carried out at the National Geoscience Research Laboratories (NGRL) in Kaduna (Federal Republic of Nigeria).

2.10. X-ray fluorescence spectrometry (XRF)

As part of this study, for the determination of the chemical composition of our samples (Arg2-B, Arg2-FNa$^+$ and Arg2-FSNa$^+$), an energy dispersive X-ray fluorescence spectrometer (EDXRF) of the "Minipal 4" model has been used. The analysis was carried out at the Kaduna NGRL.

2.11. X-ray diffraction (XRD)

In this study, for the determination of the mineralogical composition of raw red clay and its clay fractions < 2 µm, an Empyrean diffractometer DY674 (2010) with copper anode manufactured by Panalytical (Holland) was used at the Kaduna NGRL. The condition for the radiations to be in phase is expressed by Bragg's law: $n\lambda=2d_{hkl}\sin\theta$ (5). In the tube, the current was 40 mA and the voltage was 45 kV. The ICDD (International Center for Diffraction Data) PDF (Powder Diffraction File) 4 (2015) and COD (2016) databases make it easy to find and match the diffractogram to identify mineral phases and compounds.

2.12. Thermo-gravimetric Analysis (TGA)

A quantity of raw red clay was subjected to a temperature range from 28.13 °C to 950 °C with a constant rate of 10 °C per min under a nitrogen flow. The analysis was carried out at the Block B Multipurpose Laboratory of the Federal University of Technology, Mina (Federal Republic of Nigeria). The device used in this study is of the PerkinElmer MES-TGA TGA4000 brand, manufactured in the Netherlands.

2.13. Scanning electron microscopy (SEM)

In this work, the morphology of the raw red clay sample and its clay fractions was observed using a Phenom ProX type scanning electron microscope at the Laboratory of the Department of Engineering Chemistry of Ahmadu Bello University (ABU) of Zaria (Federal Republic of Nigeria). In an experimental way, the samples were placed on a double adhesive tape, then sprayed. Afterwards, they were deposited in a sputter coater (quorum-Q150R Plus E) with 5 nm gold.

2.14. Measurement of Specific surface (SS) by the Brunauer, Emmett and Teller (BET) method

In addition to the thermo-gravimetric analyses, it is quite conclusive to evaluate the SS, the pore volumes and the microporous sizes of our red clay sample. Because it is the quality and extent of these surfaces that will largely determine the adsorption capacities of this clay material. The SS of this clay material was determined at the Block B Multipurpose Laboratory of the Federal University of Technology, Mina (Federal Republic of Nigeria). These measurements were taken using a Quantachrome Nova 4200e device manufactured in the United States. The analysis was carried out after degassing the clay sample at 300 °C for 3 hours in order to desorb the water and any impurities present in the pores of the clay material.

3. Results

3.1. Preliminary analyzes of Arg2-B

Table 1 presents the results of the preliminary analysis carried out on the raw red clay (pH, CEC, humidity rate and density)

Table 1 Results of preliminary analyzes of Arg2-B

Clay	pH	CEC (meq.100 g^{-1})	H (%)	ρ ($g.cm^{-3}$)
Arg2-B	6.57	128.24	1.239	1.234

It appears from this table that Arg2-B has a slightly neutral pH in an aqueous medium, a low humidity rate with a low density. However, an increase in the mass of this clay leads to a significant regression of this pH (Figure 3). It has a high CEC of the order of 128.24 meq.100 g^{-1}. This CEC, which is the number of cations that can be substituted for the compensating cations to compensate for the negative charge of 100 g of clay, varies according to the materials.

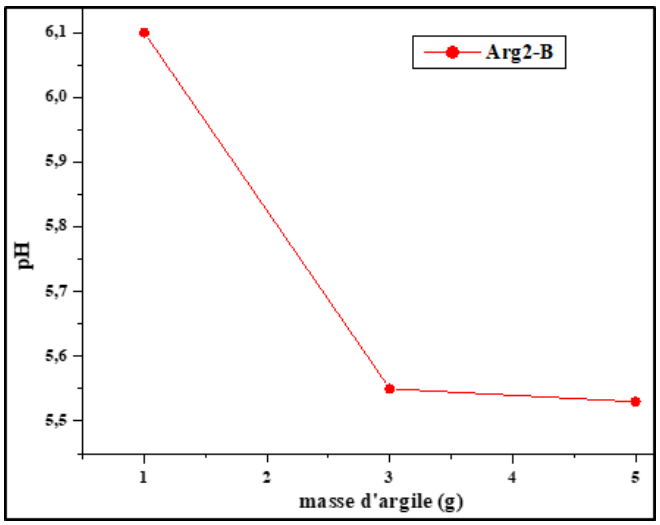

Figure 4 Variation of pH of Arg2-B as a function of mass

3.2. Isoelectric point or pH at point of zero charge (pH_{PCN})

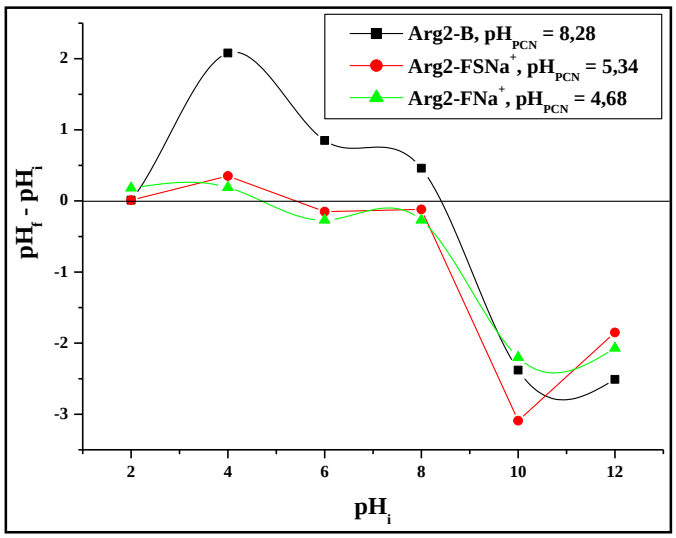

Figure 5 PH_{PCN} of Arg2-B, Arg2-$FSNa^+$ and Arg2-FNa^+

Figure 5 presents the different values of pH_{PCN} or isoelectric point of raw red clay and its clay fractions. The values are 8.28 for Arg2-B, 5.34 for Arg2-FSNa$^+$ and 4.68 for Arg2-FNa$^+$. A decrease in the pH_{PCN} of Arg2-FSNa$^+$ and of Arg2-FNa$^+$ is observed compared to that of Arg2-B. These values characterize the acidity or the alkalinity of the surface of the studied material and they are very important factors in the phenomenon of sorption especially when the electrostatic forces are implicated in the mechanism of adsorption. So for pH values lower than the pH_{PCN} found in this study the surface charge of these clays is positive, when higher it becomes negative and when equal the charges balance out, so the surface becomes electrically neutral (there is as much positive as negative charge).

3.3. X-ray fluorescence spectrometry (XRF)

The results of X-ray fluorescence analysis of raw red clay and its clay fractions are recorded in Table 2 for major oxides and loss on ignition and in Table 3 for trace elements.

Table 2 Percentages of the major oxides of Arg2-B, Arg2-FSNa$^+$ and Arg2-FNa$^+$ and those of the loss on ignition

Oxides (%)	Arg2-B	Arg2-FSNa$^+$	Arg2-FNa$^+$
SiO_2	83.2	50.1	51.3
Al_2O_3	7.04	25.7	20.2
K_2O	2,02	0.84	1.2
Na_2O	1	0.6	0.96
CaO	0.22	0.42	0.13
MgO	0.031	0.16	0.03
TiO_2	1.54	1.3	1.5
MnO	0.15	0.047	0.04
P_2O_5	ND	ND	ND
SO_3	ND	ND	ND
Fe_2O_3	3.35	4.02	5.24
LOI	0.97	15.31	16.5
SiO_2/Al_2O_3	11.2	1.9494	2.5396

ND: not detected

It appears from Table 2 that silica and alumina are the major constituent oxides in Arg2-B. The percentage of silica in this clay greatly exceeds 50%. This leads to a SiO_2/Al_2O_3 ratio equal to 11.81. So Arg2-B has a significant amount of silica. It contains a fairly large percentage of iron oxide (Fe_2O_3). It is also important to note the presence of K_2O and TiO_2 in significant quantities in this clay. Thus, the low percentages of CaO and MgO show that Arg2-B contains slightly calcium and magnesium carbonates. The low percentage of Na_2O = 1% shows that this clay contains a negligible amount of alkaline feldspars. The LOI, which is likely to estimate the rate of organic matter and carbonates contained in this clay, shows a low rate of organic matter, the value of which is less than 1%.

For the clay fractions (Arg2-FSNa$^+$ and Arg2-FNa$^+$), the silica percentages decrease considerably compared to that of Arg2-B. In addition, the Al_2O_3 percentages of these clay fractions exceed that of Arg2-B. This shows that this clay is becoming more and more aluminous. There is also a slight increase in the percentage of Fe_2O_3. However, their LOI percentages greatly exceed that of Arg2-B. In general, this clay presents important cations such as Al3$^+$, Fe^{3+}, Fe^{2+} which are potential candidates for adsorbing anions, and the SiO_2/Al_2O_3 ratio shows us the presence of several constituent minerals of this clay.

The analysis of Table 3 shows us that Arg2-B and its clay fractions present trace elements such as: V, Cr, Ni, Zn, Cu, Ga, Sr, Y, Zr, Hf, Ba, Ce, Eu, Re and Pb in ppm. Zr is the most abundant trace element in Arg2-B, followed by Sr, then V, Cu, Zn and Cr. Pb is also present in significant quantities in Arg2-B. But, in the clay fractions, the percentages of the aforementioned elements decrease, except for those of Zn, Cr and Ba which increase and especially for Ba which goes from undetected to 1000 and 1900 ppm.

Table 3 Element in trace of Arg2-B, Arg2-FSNa⁺ and Arg2-FNa⁺ in ppm

Clay	Arg2-B	Arg2-FSNa⁺	Arg2-FNa⁺
V	290.1	200.2	260
Cr	130	210.36	290.1
Ni	<0.001	<0.001	<0.001
Zn	140	200	264.06
Cu	310.1	280	260.1
Ga	7	7.63	4
Sr	310.21	370	<0.001
Y	2.6	2.9	<0.001
Zr	2490	440.3	<0.001
Hf	38.63	38.06	<0.001
Ba	ND	1900	1000
Ce	8.4	<0.001	8.3
Eu	0.25	0.19	0.18
Re	0.033	0.02	0.01
Pb	370	ND	ND

ND: not detected

3.4. X-ray diffraction (XRD)

The results of the mineralogical analyzes carried out on the raw clay and its clay fractions by X-ray diffraction are given in the figures below. These figures, after indexing the set of peaks of each phase by the ICDD and COD database, show the following observations:

Arg2-B consists of montmorillonite, kaolinite, illite, rutile and quartz. The characteristic peaks of montmorillonite at 2θ = 7.93°, 19.76°, 34.92°, 35.90°, 36.42°, 38.02°, 40.49°, 41.31°, 45 ,63°, 50.36°, 54.89°, 55.32°, 59.62°, 62.38°, 63.89°, 67.61° and 68.09° correspond respectively to the reticular distances 10, 82Å, 4.46Å, 2.56Å, 2.50Å, 2.45Å, 2.37Å, 2.23Å, 2.12Å, 1.98Å, 1.81Å, 1, 67Å, 1.65Å, 1.54Å, 1.48Å, 1.45Å, 1.38Å and 1.37Å (file: 96-901-0960). This montmorillonite has the chemical formula $Si_{7.8}Al_{1.72}Cs_{0.16}Fe_{0.20}Mg_{0.28}O_{20}$. Kaolinite is characterized by peaks at 2θ = 12.39°, 19.85°, 24.94°, 34.99°, 35.95°, 37.80°, 38.52°, 40.38°, 42.41°, 45.67°, 47.23°, 50.33°, 54.96°, 55.34°, 59.97°, 62.29°, 63.98°, 65.84°, and 68.35° corresponding respectively to the reticular distances 7.14 Å, 4.46 Å, 3.57 Å, 2.56 Å, 2.50 Å, 2.38 Å, 2.33 Å, 2.12 Å, 1.98Å, 1.81Å, 1.67Å, 1.65Å, 1.54Å, 1.48Å, 1.45Å, 1.41Å and 1.37Å (file: 96-900 -9235). Illite peaks are observable at 2θ = 8.82°, 17.69°, 19.75°, 21.62°, 23.3°, 30.55°, 34.97°, 35.82°, 36.82°, 38.11°, 40.13°, 45.36°, 49.92°, 55.58°, 59.72°, 62.29°, 67.62° and 68.31° corresponding respectively to the reticular distances 9.88 Å, 4.97 Å, 4.46 Å, 3.98 Å, 3.82 Å, 2.90 Å, 2.56 Å, 2.50 Å, 2.45 Å, 2.37Å, 2.23Å, 1.98Å, 1.85Å, 1.81Å, 1.65Å, 1.54Å, 1.48Å, 1.38Å and 1.37Å (file: 96-901-3719). The characteristic peaks of rutile at 2θ = 27.43°, 64.04° and 65.5° correspond to lattice distances 3.24 Å, 1.45 Å and 1.41 Å (file: 96-900-7433), those of quartz at 2θ = 21.19°, 27.02°, 37.15°, 39.99°, 55.72° and 68.88° correspond respectively to the reticular distances 4.26 Å, 3.33 Å, 2.45Å, 2.25Å, 1.65Å and 1.37Å (file: 96-900-0777).

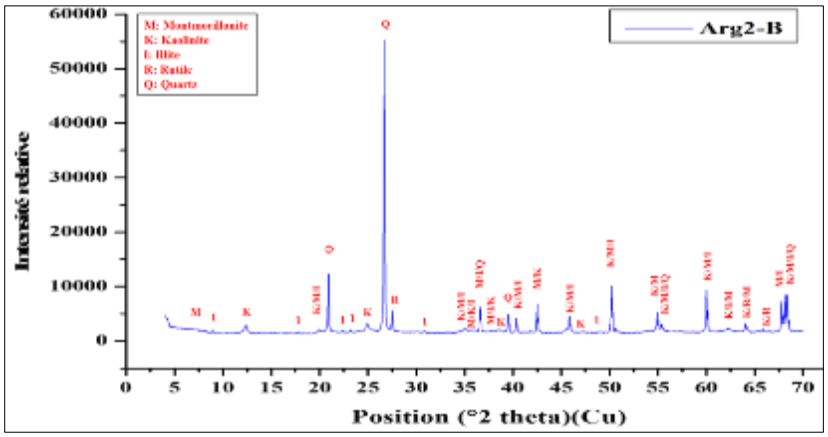

Figure 6 Diffractogram of Arg2-B

Arg2-FSNa⁺ always presents characteristic peaks of kaolinite, montmorillonite and illite with more intensities than in the raw clay and the disappearance of the rutile peaks. The quartz peaks remain persistent, but with low intensities.

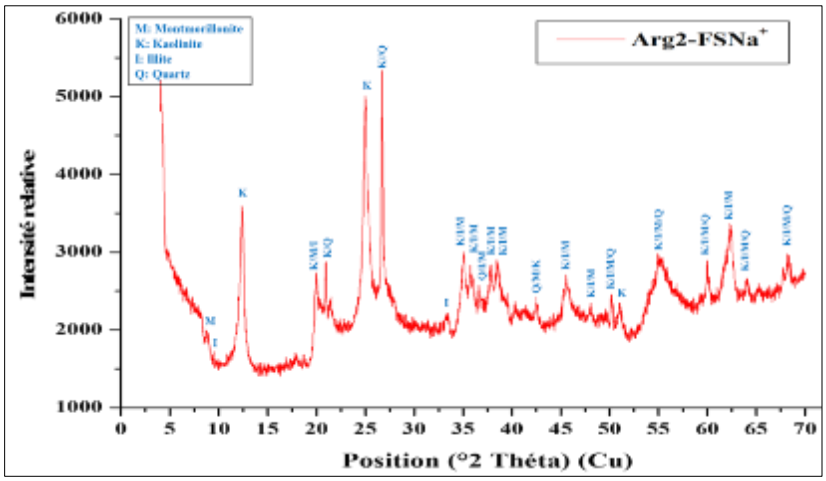

Figure 7 Diffractogram of Arg2-FSNa⁺

Arg2-FNa⁺ still retains the same minerals as before, but with a decrease in the intensity of the peaks and appearance of a new halite peak at 2θ = 31.7° corresponding to a reticular distance of 2.81 Å (file: 96-900-3309).

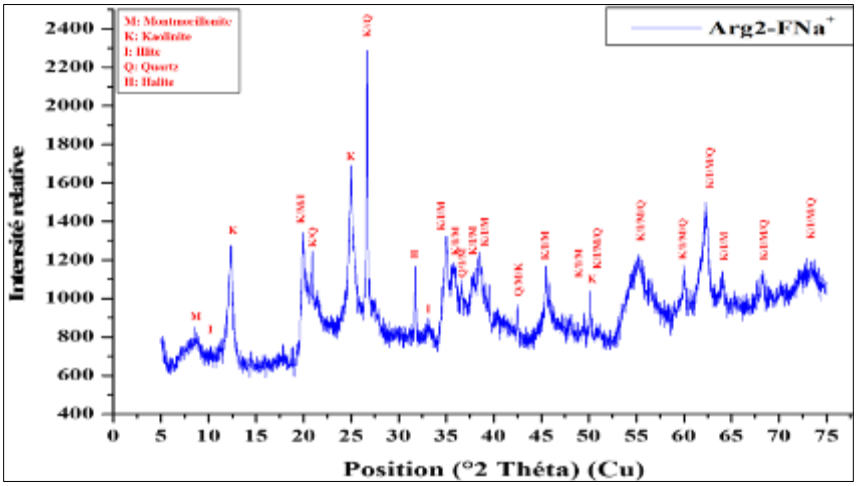

Figure 8 Diffractogram of Arg2-FNa⁺

3.5. Thermo-gravimetric Analysis (TGA)

The result of the thermo-gravimetric analysis carried out on Arg2-B is presented in Figure 9. This Figure (TGA curve) shows five observable mass losses between 28.15 and 369.31 °C (with a loss of 37.432%), between 369.31 and 536.59 °C (with a loss of 42.439%), between 536.59 and 659.41 °C (with a loss of 2.904%), between 668.17 and 676.07 °C (with a loss of 0.567%) and between 760.49 and 884.14 °C (with a loss of 1.037%). A weight increase is perceptible on the TGA curve between 659.41 and 668.17 °C and between 676.07 and 760.49 °C. The derivative of the TGA curve (DTG) shows five endothermic peaks (at 318.26 °C, at 353.46 °C, at 477.08 °C, at 670.35 °C and at 730.37 °C) and 2 exothermic peaks (at 658.65 °C and at 679.73 °C).

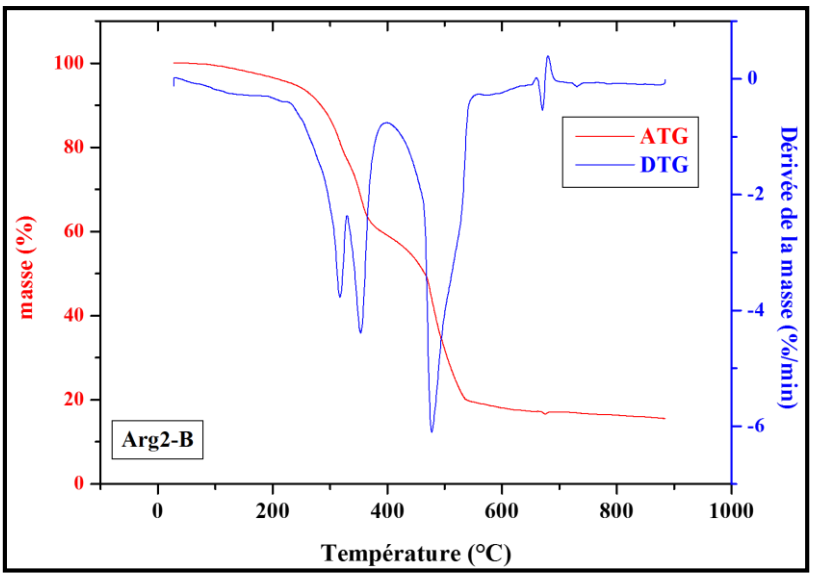

Figure 9 ATG and DTG curve of Arg2-B

3.6. Measurement of SS by the Brunauer, Emmett and Teller (BET) method

Table 4 presents the SS of Arg2-B calculated according to the methods.

Table 4 Different surfaces of Arg2-B

Characteristic	Sizes	Arg2-B
Specific surface ($m^2.g^{-1}$)	at P/P0 = 0.3	326.6
	BET	418.4
	Langmuir	967.7
	Cumulative (BJH)	507.8
	Cumulative (DH)	538
	External (t-method)	418.4
	Micropores (DR)	540
	Cumulative (DFT)	144.4

The analysis of this table shows a variability of the SS according to the methods used. At one point (P/P0 = 0.3), Arg2-B exhibits a very large SS, but it is lower than that found by BET. A very high value was obtained by the Langmuir method of around 967.7 $m^2.g^{-1}$. Regarding the cumulative SS according to the methods (BJH and DH), the difference is not significant, but it greatly exceeds that of BET and remains below that of Langmuir. The external SS determined by t-method is the same as that of BET, while the microporous one determined by DR method slightly exceeds it. As for the DFT method, it shows a value of the SS which is much lower than the values found for the other methods.

Table 5 summarizes the results of the Arg2-B pore volumes calculated according to the different methods.

Table 5 Pore volumes of Arg2-B

Characteristic	Sizes	Arg2-B
Volume ($cm^3.g^{-1}$)	BJH (cumulative)	0.2487
	DH (cumulative)	0.2535
	DR (micropore)	0.1919
	HK (micropore)	0.0981
	SF (micro-pore)	0.0389
	DFT (cumulative)	0.155

It can be seen from this table that the cumulative pore volumes according to the BJH and DH methods do not show a significant difference, but they greatly exceed that calculated according to the DFT method. While the microporous volumes according to the shapes of the pores by the HK and SF methods show a very significant difference. That of HK (0.0981 $cm^3.g^{-1}$) corresponding to the slit-like shape is widely higher than that of SF (0.0389 $cm^3.g^{-1}$) corresponding to the cylindrical-like shape. But, they are lower than that calculated according to the DR method.

Table 6 presents the results of the distribution of the sizes of pores calculated according to the various methods.

Table 6 Pore size of Arg2-B according to the different methods

Characteristic	Sizes	Arg2-B
Pore size (nm)	Mean diameter BJH	2.413
	Average diameter DH	2.413
	Pore width DR	5.423
	Pore diameter DA	2.66
	Pore diameter HK	0.3675
	Pore diameter SF	0.4523
	Pore diameter DFT	2.647

Analysis of this table shows that the average pore size diameter according to the BJH and DH methods by adsorption is the same, with a good pore width calculated according to the DR method and a micro-pore diameter according to the DA method similar to that calculated by the DFT method which is the best method allowing a much more precise approach to pore size. Because it includes the size of micro-pores and narrow mesopores which other methods cannot determine. Thus, the microporous diameter size according to the HK and SF methods which take into account the pore shape, shows a small difference in pore size between these two methods. That of SF (0.4523 nm) slightly exceeds that of HK (0.3675 nm).

3.7. Scanning electron microscopy (SEM)

SEM was used to observe the morphology and organization of clay particle aggregates. The images obtained from the red clay and its clay fractions are presented in Figure 10. The micrographs show that this clay has morphologies showing crystals of irregular shape distributed in a random manner. No significant difference was observed between Arg2-B and its clay fractions. Given the diversity of minerals identified contained in these clay particles by XRD and the low resolution of the SEM image of this clay, the structural identification of the morphologies specific to the basic clay minerals (Montmorillonite, Kaolinite, Illite) remains very difficult. But, it shows the degree of crystallinity of this clay material.

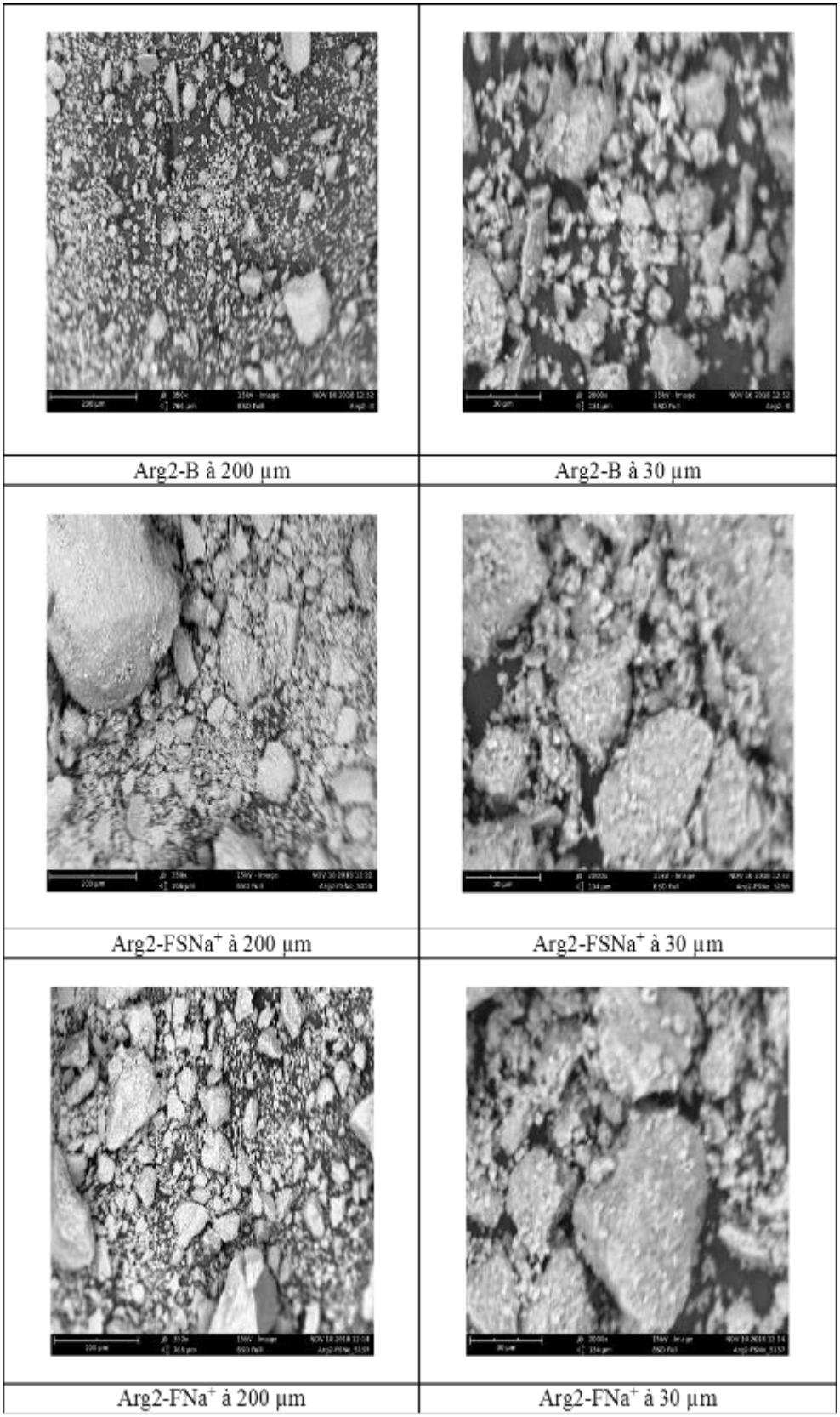

Figure 10 SEM images of Arg2-B, Arg2-FSNa+ and Arg2-FNa+

4. Discussion

4.1. Preliminary analyzes of red clay (Arg2-B)

The pH value obtained for Arg2-B shows that it has surfaces which are made up of acid groups capable of reacting with the hydroxyl groups of water, which will lead to an increase in H^+ ions in the medium, which is zero. doubt prone to lower pH. The value obtained is lower than those obtained by, *Zahaf*, *Bouzid*, *Amin and al* and *Qlihaa and al*, [9, 10, 13, 14]. This difference could be due to the low levels of alkaline and alkaline earth cations possessed by Arg2-B, which is confirmed by the results of the X-ray fluorescence analysis. On the other hand, the value obtained is almost similar to that obtained by *Maman and al* on the LP11, but greatly exceeds that obtained by the same author on the T10 in Tillabéry region in Niger [6]. The low humidity rate recorded for Arg2-B could be due to the arid nature of the area where this clay was taken and shows its non-hygroscopic character, which is also confirmed by the results of the ATG-DTG. It appears from the literature that the CEC of between 3 to 15 meq.100 g^{-1} corresponds to kaolinite, from 10 to 40 meq.100 g^{-1} to illite, from 80 to 150 to smectites [15]. So the CEC of our raw clay determined which is 128.24 meq.g^{-1} belongs to the interval of 80 to 150 meq.g-1, which lets us suggest that it contains a significant amount of minerals belonging to the smectite family. The density obtained is below that obtained by *Bouzid* [9]. This could be due to the geological formation or the experimental conditions (mesh, method) which differ, or our clay does not contain a dense element (such as quartz) likely to increase this density.

4.2. pH at the point of zero charges (pH_{PCN})

The pH_{PCN} of Arg2-B obtained in this study is almost similar to those in the literature for smectitic clays [16]. This lets us suggest that Arg2-B still contains significant amounts of minerals belonging to the smectite family. This corroborates the hypothesis put forward above in the case of the CEC. The decrease in pH_{PCN} of the clay fraction (Arg2-$FSNa^+$ and Arg2-FNa^+) would be mainly due to the elimination of certain impurities carrying negative charges which are likely to increase this pH_{PCN} in the raw state. However, the decrease in pH_{PCN} observed in the case of Arg2-FNa^+ would probably be due to the adsorption of Na^+ by the negative charges of these clay fractions.

4.3. X-ray fluorescence spectrometry (XRF)

The high percentage of silica recorded in Arg2-B could be mainly attributable to clay minerals and quartz. It appears from the literature that SiO_2/Al_2O_3 ratios between 2 and 5.5 generally correspond to materials of type 2/1, more precisely montmorillonite [17, 18]. So this already suggests that Arg2-B could contain montmorillonite in large quantities and in addition to montmorillonite, it could also contain other minerals in significant quantities such as quartz whose main constituent is silica. This is in agreement with the various hypotheses put forward above. So this hypothesis will be confirmed or invalidated later by X-ray analyses. The fairly large percentage of Fe_2O_3 recorded in Arg2-B could be due to the existence of minerals that can contain iron in large quantities, because according to the literature, iron is found in the form of oxide-hydroxides, namely goethite, and/or oxides such as hematite and magnetite [19, 20]. So, drawing on this result from the literature, we can say that Arg2-B could contain goethite and / or hematite and magnetite. These types of minerals are generally attributable to illites and montmorillonites. So in addition to the montmorillonite mentioned above, Arg2-B could also contain illites. The potassium content recorded could be attributable to illites while that of titanium attributable to kaolinites, since it appears from the literature that titanium is found in the form of rutile or anatase in kaolinitic clays [8]. This lets us suggest that Arg2-B in addition to montmorillonite and illite, could contain kaolinite. The low percentages of CaO and MgO recorded let us predict that Arg2-B is devoid of carbonated elements. The low DPF percentage of Arg2-B shows that it contains only a minimal amount of organic matter and carbonates.

The decrease in silica in the clay fractions (Arg2-$FSNa^+$, Arg2-FNa^+) compared to the raw state, would be due to the fact that this silica could only come from the constituent minerals of this clay except that of quartz. This shows that this clay is becoming more and more aluminous. On the other hand, the increase in the percentage of Al_2O_3 of the clay fractions compared to that of Arg2-B could be attributable to the aluminous minerals which are less dense than the siliceous minerals. In addition, the increase in the percentage of LOI of these clay fractions greatly exceeding that of Arg2-B, this shows that the extraction of the clay fraction was well carried out and that it only contains fractions rich in clay minerals which are capable of adsorbing large quantities of water, of which after calcination this water is easily desorbable, which could give them a high SS. The presence of the trace elements found (V, Cr, Ni, Zn, Cu, Ga, Sr, Y, Zr, Hf, Ba, Ce, Eu, Re and Pb) in this study differs from the results found by *Gourouza* [21] in Niger in the clays of Tahoua region, where he concludes the total absence of these elements. This could be due to the difference in the geological formations where these samples were taken. But, more than 40 trace elements were found by *Amin and al* [13] in Ivory Coast in UB1 and UB2 clays. This is in agreement with the results of the present study. And he concludes that UB1 contains kaolinite and illite and UB2 contains montmorillonite and illite. This leaves us to suggest that our clay could contain all these minerals.

4.4. X-ray diffraction (XRD)

XRD analysis showed that Arg2-B contains a mixture of clay minerals with impurities. Montmorillonite, kaolinite and illite are the main constituent minerals together with impurities such as quartz and rutile. This proves the heterogeneous character of Arg2-B, which is in perfect agreement with the various observations made at the SEM and the X-ray fluorescence results. impurities such as quartz and goethite, and smectitic type associated with rutile [8, 9, 22, 23]. The main constituent minerals in the clay fractions (Arg2-FSNa$^+$ and Arg2-FNa$^+$) are montmorillonite, kaolinite and illite which appear with very intense peaks, but with the persistence of some low intensity peaks characteristic of quartz. These results are in agreement with those of several authors who reported the presence of quartz in the clay fractions [8, 14, 24]. So these different observations confirm the significant elimination of quartz during the extraction of the clay fraction, these results also confirm those of X-ray fluorescence.

4.5. Thermo-gravimetric analysis

In the case of Arg2-B, the 1st loss could be attributable to the dehydration of the adsorbed water and the water bound to the interfoliar cations. This strong dehydration leads us to suggest that this clay was largely made up of swelling materials of the smectitic type (montmorillonite) [25]. The 2nd loss of mass could be attributable to the dehydroxylation of montmorillonite or that of Kaolinite which can be transformed into metakaolinite. The 3rd and 4th mass losses could be attributable to the dehydroxylation of montmorillonite and illite, each leading to a structural reorganization of the network with the appearance of perceptible weight increases on the TGA curve and exothermic peaks on the DTG curve. The latter mass loss could be attributable to the dehydroxylation of iron- and aluminum-bound OH of illite because according to the literature, the dehydroxylation of illite is accompanied up to 800 °C. These hypotheses could be supported by the XRD results.

4.6. Measurement of SS by the Brunauer, Emmett and Teller (BET) method

The SS obtained by the different methods of Arg2-B except those of Langmuir, single point and DFT, do not reach that of a pure montmorillonite (880 $m^2.g^{-1}$), but largely exceed that of illite pure (between 100 and 175 $m^2.g^{-1}$) and that of pure kaolinite (between 10 and 30 $m^2.g^{-1}$). These SS obtained not reaching that of a pure montmorillonite could be due to the presence of illite, kaolinite and impurities contained in Arg2-B which are likely to attenuate the normal development of the SS of a montmorillonite. These results are in agreement with those of the XRD which showed the presence of Kaolinites, illites and impurities in Arg2-B. Similarly, the values exceeding those of kaolinite and illites could be due to the presence of montmorillonite and impurities which could increase these SS. This is always confirmed by the results of the XRD. This leads us to suggest that Arg2-B mainly contains montmorillonite. In addition, the values obtained in this study greatly exceed those found by many authors [10, 21, 22, 24, 26, 27, 28]. These obtained strong SS could make Arg2-B a high performance adsorbent material capable of adsorbing both anions and cations. Thus, the differences observed between the different methods, especially that of Langmuir and BET, could be attributable to the different assumptions that each of the methods is based on. The high Langmuir SS obtained of 967.4 $m^2.g^{-1}$ would probably be due to the three assumptions that this model uses (adsorption is localized and only gives rise to the formation of a monolayer; all the sites are equivalent and the surface is uniform; no interaction between the adsorbed molecules). This stipulates that there is no distinction between the different pores of this clay material (micro, meso and macropore). So as Arg2-B is made up of several kinds of minerals (montmorillonite, kaolinite and illite) with impurities (rutile, quartz and other elements), it could lead to the adsorption of large amount of nitrogen gas in the different pores that Arg2-B contains, which will undoubtedly lead to the exceptional enhancement of the SS of Arg2-B greatly exceeding that of BET. These strong SS could increase the performance of Arg2-B. Results for Langmuir's SS for clay materials are somewhat lacking to our knowledge in the literature.

The total pore volumes found by the methods (BJH and DH) are greater than those obtained by *Bouna* and by *Célini* [24, 27] respectively on montmorillonite, on crude and soda TAG. This could be due to the fact that Arg2-B consists of several minerals likely to increase the pore volume, which is confirmed by the SS obtained in this study which largely exceed those of these authors. Similarly, the micro-pore volume of Arg2-B exceeds that of *Gourouza and al*, *Bouna* and *Haffane and al* [7, 24, 28]. The assumption is the same as before.

The results obtained by the different methods show that the pore sizes of Arg2-B are on the one hand less than 2 nm characteristic of microporous materials, and on the other hand greater than 2 nm but not reaching 50 nm characteristic of microporous materials. mesoporous materials according to the UIPCA classification. This suggests to us that Arg2-B could contain micro-pores and mesopores. But, according to the DFT method which gives the results of micro-pores and mesopores, shows a large peak at a diameter size of less than 2 nm confirming the presence of micro-pores and two peaks at diameter sizes greater than 2 nm confirming the presence mesopores. These hypotheses could also be confirmed by the obtained microporous SS largely exceeding that of BET. Furthermore, the diameter sizes obtained by

the HK and SF methods and according to the pore width, let us think that Arg2-B could contain slit-shaped and cylindrical-shaped micro-pores, because the values obtained according to these two methods are lower. at 2 nm. This further shows that Arg2-B could contain more micro-pores than mesopores. This hypothesis could be supported on the one hand by its high microporous SS and on the other hand by its high microporous volume. The diameter size values obtained in this study are lower than those of *Bouna* [24]. This could probably be due to the multiplicity of minerals and impurities contained in Arg2-B on the one hand or to the large SS developed by this clay on the other.

4.7. Scanning electron microscopy (SEM)

The rather irregular morphologies observed on the SEM images of Arg2-B could be largely attributable to smectitic-type materials (montmorillonite) [29]. Thus, the particles of variable size and dimension perceptible on the X-rays could be attributable to illite [29]. Similarly, small particles of hexagonal shape and sometimes reduced to diamonds could be attributed to kaolinites [29, 30]. The rough deposits visible on the crystals could be free silicas in this clay material and *Bellaroui* and *Mokhtari* impurities *in* [31]. These hypotheses are in agreement with the results of XRD, X-ray fluorescence and ATG-DTG.

5. Conclusion

Ultimately, the red clay characterized by the different techniques consists of montmorillonite, illite and kaolinite associated with impurities such as quartz and rutile. It exhibits a high degree of crystallinity with large specific surface areas, slit and cylindrical micropore volumes and large pore sizes. It is also slightly neutral with trace elements and a basic isoelectric point. These characters give this clay very impressive intrinsic properties allowing its use in water treatment.

Compliance with ethical standards

Acknowledgments

Our thanks go to the heads of the Departmental Directorate of hydraulics and sanitation of Tanout, for providing us with the equipment necessary for the realization of this work.

Disclosure of conflict of interest

The authors declare that they have no competing interests.

References

[1] Rabilou SOULEY MOUSSA, Maman Mousbahou MALAM ALMA, Mahaman Sani LAOUALI, Ibrahim NATATOU and HABOU Issa. Physico-chemical characterization of the waters of the Continental Intercalaire / Hamadien and Continentalsiems Terminal aquifers in the Zinder region (Niger). Int. J. Biol. Chem. Science. 2018; 12(5):2395-2411.

[2] Souley Moussa Rabilou, Malam Alma Maman Mousbahou, Mahaman Sani Laouali, Natatou Ibrahim, Issa Habou. Physico-chemical characterization of groundwater in the basement of the Zinder region (Niger) during the rainy season and the dry season. European Scientific Journal. 2018; 14(27): 317-345.

[3] Rabilou SOULEY MOUSSA, Maman Mousbahou MALAM ALMA, Mahaman Sani LAOUALI, Ibrahim NATATOU and Issa HABOU. Comparative study of the physico-chemical quality of Korama aquifer waters (superficial Korama and deep Korama) in the Zinder region (Niger) during the rainy season and the dry season. Africa SCIENCE. 2018; 14(6) 203 – 215.

[4] World Health Organization (WHO) and UNICEF. Joint Monitoring Program (JMP) 2017.

[5] Gourouza, M., Natatou, I., Bayo, K. and Boos, A. Study of the adsorption of fluoride ions by a bentonite from Niger. J. Soc. West-Afr. Chem. 2013; 036: 15-20.

[6] Maazou AM, Adamou R, Konaté M, Alassane A, Adel M. Valorization of two clay materials from the Niger River valley in the elimination of copper from drinking water. J. Soc. West-Afr. Chem. 2017; 043: 64 – 75

[7] Marou G, Adamou Z, Ibrahim N, Anne B. Characterization of a mixed clay from Niger. Rev. CAMES – Sciences Struct. Mast. 2013; 1: 29-39.

[8] Zaki O, Abdoulaye A, Nomao DL, Rumari P, Palomino GT, Amadou I. Characterization of Soils in Irrigated Perimeters of Western Niger by X-ray Diffraction. J.Soc. West-Afr. Chem. 2008; 026: 89-97.

[9] Bouzid S. Adsorption of organic pollutants on a clay exchanged with phosphoniums. [Doctoral thesis]. University of Science and Technology of Oran Mohamed Boudiaf. Option physico-chemistry of mineral materials; 2015.

[10] Zahaf F. Structural study of modified clays applied to the adsorption of pollutants [PhD thesis]. Mustapha Stambouli University of Mascara. Speciality: Materials Chemistry; 2017.

[11] NF P 94 050: Determination of the water content by weight of materials. Steaming method.

[12] DERAFA G. Synthesis and characterization of modified montmorillonite: Application to the adsorption of cationic dyes [Memory of Magister]. University Ferhat Abbas-Setif-1-. Option: Chemical Engineering; 2014

[13] Amin NC, Andji YYJ, Ake M., Yolou SF, Toure-Abba A, Kra G. Mineralogy and physicochemistry of Buruli ulcer treatment clays in Ivory Coast. J. sci. pharm. biol. 2009; 10(1): 21-30

[14] Qlihaa A, Dhimni S, Melrhaka F, SRhiri A. Physicochemical characterization of Moroccan clay. J.Mater.Environ.Sci. 2016; 7(5): 1741-1750.

[15] Abidi N. Interactions between natural clays and dyer effluents. Influence of clay surface properties and dye adsorption mechanisms [PhD thesis]. University of Strasbourg. Specialty: Geochemistry and Environment; 2015.

[16] Tombacz E, Szekeres M. Colloidal behavior of aqueous montmorillonite suspensions: the specific role of pH in the presence of indifferent electrolutes. Applied Clay Science. 2004 ; 27: 75-94.

[17] Jozja N, Baillif P, Touray JS, Pons CH, Muller F, Burgevin C. Multi-scale impacts of a (Mg, Ca)–Pb exchange and its consequences on the increase in permeability of a bentonite . Geoscience Reports. 2003; 335: 729-736.

[18] Chouchane T, Chouchane S, Boukari A. Elimination of manganese in solution by kaolin, kinetic and thermodynamic study. Journal of Renewable Energies. 2013; 16: 313-335.

[19] Sei J, Jumas JC, Olivier-Fourcade J, Quiquampoix H, Straunton S. Clays and Clay minerals. 2002; 50, 212.

[20] Soro NS, Blanchart P, Aldon L, Olivier-Fourcade J, Jumas JM, Bonnet JP. Journal of American Ceramic Society. 2003; 86:129.

[21] Gourouza M. Characterization of Materials (Clays, Gypsum and Calcined Bones); Quantitative, kinetic and thermodynamic study of the adsorption of fluoride ions by Sabon-Karré clay and by calcined beef bones [PhD thesis]. Abdou Moumouni University of Niamey; 2012.

[22] Errais E. Surface reactivity of natural clays Study of the adsorption of anionic dyes [PhD thesis]. University of Strasbourg. Speciality ; Environmental Geochemistry; 2011.

[23] Zghal HB, Mhiri MMT. Physicochemical and mechanical characterization of ceramic materials obtained from Tunisian clays. Glasses, Ceramics & Composites. 2011; 1(2): 25-33.

[24] Bouna L. Functionalization of clay minerals of Moroccan origin by TiO2 for the elimination by photocatalysis of organic micropollutants from aqueous media [PhD thesis]. University of Toulouse, Discipline or specialty: Materials science and engineering; 2012.

[25] Villieras F. Study of changes in the properties of talc and chlorite by heat treatment. [Doctoral thesis]. National Polytechnic Institute of Lorraine. Geosciences-Raw Materials option; 1993.

[26] Bouras O. Adsorbent Properties of Organophilic Bridged Clays: Synthesis and Characterization [PhD thesis]. University of Limoges, Discipline: Water Chemistry and Microbiology; 2003.

[27] Célini N. Treatment of clays by cold plasma for their use as fillers of clay-polymer nanocomposites. [Doctoral thesis] University of Maine. Specialty in chemistry and physico-chemistry of polymers; 2004.

[28] Soukaina H, Ouafae A, Tarik C. Study of the effect of purification and modification of a local clay on its structural and textural properties (Investigation of the effect of purification and modification of a local clay on its structural and textural properties). J. Mater. About. Science. 2016; 7(2): 525-530.

[29] Konan KL. Interactions between clay materials and some basic medium rich in calcium. [Doctoral thesis]. University of Limoges. Specialty: Ceramic Materials and Surface Treatments; 2006.

[30] Perrin S. Modeling the kinetics of non-isothermal and (or) non-isobaric transformations. Application to the dehydroxylation of kaolinite and to the reduction of triuranium octoxide by hydrogen [PhD thesis]. National School of Mines of Saint-Etienne. Speciality: process engineering; 2002.

[31] Djebbar M. Maghnia clay: purification and adsorption of pollutants. [Doctoral thesis]. University of Oran, Option: materials chemistry; 2014.